

# Measurements of $\gamma/\phi_3$ at B factories

A. Poluektov  
 Budker Institute of Nuclear Physics, Novosibirsk, Russia

This report summarizes the most recent progress in measuring the angle  $\gamma$  (or  $\phi_3$ ) of the Unitarity Triangle.

## 1. Introduction

Measurements of the Unitarity Triangle parameters allow to search for New Physics effects at low energies. Most of such measurements are currently performed at  $B$  factories — the  $e^+e^-$  machines operated with the center-of-mass energy around 10 GeV at  $\Upsilon(4S)$  resonance, which primarily decays to  $B$  meson pairs.

One angle,  $\phi_1$  (or  $\beta$ )<sup>1</sup>, has been measured with high precision at BaBar [1] and Belle [2] experiments. The measurement of the angle  $\phi_2/\alpha$  is more difficult due to theoretical uncertainties in calculation of the penguin diagram contribution. Precise determination of the third angle,  $\phi_3/\gamma$ , is possible, *e.g.*, in the decays  $B^\pm \rightarrow DK^\pm$ . Although it requires a lot more data than for the other angles, it is theoretically clean due to the absence of loop contributions. In the recent years, a lot of progress has been achieved in the methods of the precise determination of the  $\phi_2$  and  $\phi_3$  angles. This report summarizes the most recent progress in measuring the angle  $\phi_3/\gamma$ .

## 2. GLW analyses

The technique of measuring  $\phi_3$  proposed by Gronau, London and Wyler (and called GLW) [3] makes use of  $D^0$  decays to CP eigenstates, such as  $K^+K^-$ ,  $\pi^+\pi^-$  (CP-even) or  $K_S^0\pi^0$ ,  $K_S^0\phi$  (CP-odd). Since both  $D^0$  and  $\bar{D}^0$  can decay into the same CP eigenstate ( $D_{CP}$ , or  $D_1$  for a CP-even state and  $D_2$  for a CP-odd state), the  $b \rightarrow c$  and  $b \rightarrow u$  processes shown in Fig. 1 interfere in the  $B^\pm \rightarrow D_{CP}K^\pm$  decay channel. This interference may lead to direct CP violation. To measure  $D$  meson decays to CP eigenstates a large number of  $B$  meson decays is required since the branching fractions to these modes are of order 1%. To extract  $\phi_3$  using the GLW method, the following observables sensitive to CP violation are used: the

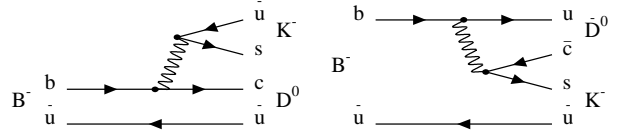


Figure 1: Feynman diagrams for  $B^- \rightarrow D^0 K^-$  and  $B^- \rightarrow \bar{D}^0 K^-$ .

asymmetries

$$\begin{aligned} \mathcal{A}_{1,2} &\equiv \frac{\mathcal{B}(B^- \rightarrow D_{1,2}K^-) - \mathcal{B}(B^+ \rightarrow D_{1,2}K^+)}{\mathcal{B}(B^- \rightarrow D_{1,2}K^-) + \mathcal{B}(B^+ \rightarrow D_{1,2}K^+)} \\ &= \frac{2r_B \sin \delta' \sin \phi_3}{1 + r_B^2 + 2r_B \cos \delta' \cos \phi_3} \end{aligned} \quad (1)$$

and the double ratios

$$\begin{aligned} \mathcal{R}_{1,2} &\equiv \frac{\mathcal{B}(B^- \rightarrow D_{1,2}K^-) + \mathcal{B}(B^+ \rightarrow D_{1,2}K^+)}{\mathcal{B}(B^- \rightarrow D^0K^-) + \mathcal{B}(B^+ \rightarrow D^0K^+)} \\ &= 1 + r_B^2 + 2r_B \cos \delta' \cos \phi_3, \end{aligned} \quad (2)$$

where

$$\delta' = \begin{cases} \delta_B & \text{for } D_1 \\ \delta_B + \pi & \text{for } D_2 \end{cases}, \quad (3)$$

and  $r_B \equiv |A(B^- \rightarrow \bar{D}^0 K^-)/A(B^- \rightarrow D^0 K^-)|$  is the ratio of the magnitudes of the two tree diagrams shown in Fig. 1,  $\delta_B$  is their strong-phase difference. The value of  $r_B$  is given by the ratio of the CKM matrix elements  $|V_{ub}^* V_{cs}|/|V_{cb}^* V_{us}| \sim 0.38$  and the color suppression factor. Here we assume that mixing and CP violation in the neutral  $D$  meson system can be neglected.

Instead of four observables  $\mathcal{R}_{1,2}$  and  $\mathcal{A}_{1,2}$ , only three of which are independent (since  $\mathcal{A}_1 \mathcal{R}_1 = -\mathcal{A}_2 \mathcal{R}_2$ ), an alternative set of three parameters can be used:

$$\begin{aligned} x_\pm &= r_B \cos(\delta_B \pm \phi_3) \\ &= \frac{\mathcal{R}_1(1 + \mathcal{A}_1) - \mathcal{R}_2(1 + \mathcal{A}_2)}{4}, \end{aligned} \quad (4)$$

and

$$r_B^2 = \frac{\mathcal{R}_1 + \mathcal{R}_2 + 2}{2}. \quad (5)$$

The use of these observables allows for a direct comparison with the methods involving Dalitz plot analyses of  $D^0$  (see Section 4), where the same parameters  $x_\pm$  are obtained.

<sup>1</sup>Two different notations of the Unitarity Triangle are used:  $\alpha$ ,  $\beta$ ,  $\gamma$  or  $\phi_2$ ,  $\phi_1$  and  $\phi_3$ , respectively. The second option (adopted by Belle collaboration) will be used throughout the paper except for the case when BaBar results are discussed.

Table I Results of the GLW analysis by BaBar

$\mathcal{R}_1$	$1.06 \pm 0.10 \pm 0.05$
$\mathcal{R}_2$	$1.03 \pm 0.10 \pm 0.05$
$\mathcal{A}_1$	$+0.27 \pm 0.09 \pm 0.04$
$\mathcal{A}_2$	$-0.09 \pm 0.09 \pm 0.02$
$x_+$	$-0.09 \pm 0.05 \pm 0.02$
$x_-$	$+0.10 \pm 0.05 \pm 0.03$
$r_B^2$	$0.05 \pm 0.07 \pm 0.03$

Measurements of  $B \rightarrow D_{CP}K$  decays have been performed by both the BaBar [4] and Belle [5] collaborations. Recently, BaBar updated their GLW analysis using the data sample of 382M  $B\bar{B}$  pairs [6]. The analysis uses  $D^0$  decays to  $K^+K^-$  and  $\pi^+\pi^-$  as  $CP$ -even modes,  $K_S^0\pi^0$  and  $K_S^0\omega$  as  $CP$ -odd modes.

The results of the analysis (both in terms of asymmetries and double ratios, and alternative  $x_{\pm}, r_B^2$  set) are shown in Table I. As follows from (1) and (3), the signs of the  $\mathcal{A}_1$  and  $\mathcal{A}_2$  asymmetries should be opposite, which is confirmed by the experiment. The  $x_{\pm}$  values are in a good agreement with the ones obtained by Dalitz analysis technique.

### 3. ADS analyses

The difficulties in the application of the GLW methods arise primarily due to the small magnitude of the  $CP$  asymmetry of the  $B^{\pm} \rightarrow D_{CP}K^{\pm}$  decay probabilities, which may lead to significant systematic uncertainties in the observation of the  $CP$  violation. An alternative approach was proposed by Atwood, Duniety and Soni [7]. Instead of using the  $D^0$  decays to  $CP$  eigenstates, the ADS method uses Cabibbo-favored and doubly Cabibbo-suppressed decays:  $\bar{D}^0 \rightarrow K^-\pi^+$  and  $D^0 \rightarrow K^-\pi^+$ . In the decays  $B^+ \rightarrow [K^-\pi^+]_D K^+$  and  $B^- \rightarrow [K^+\pi^-]_D K^-$ , the suppressed  $B$  decay corresponds to the Cabibbo-allowed  $D^0$  decay, and vice versa. Therefore, the interfering amplitudes are of similar magnitudes, and one can expect the significant  $CP$  asymmetry.

Unfortunately, the branching ratios of the decays mentioned above are so small that they cannot be observed using the current experimental statistics. The observable that is measured in the ADS method is the fraction of the suppressed and allowed branching ratios:

$$\begin{aligned} \mathcal{R}_{ADS} &= \frac{Br(B^{\pm} \rightarrow [K^{\mp}\pi^{\pm}]_D K^{\pm})}{Br(B^{\pm} \rightarrow [K^{\pm}\pi^{\mp}]_D K^{\pm})} \\ &= r_B^2 + r_D^2 + 2r_B r_D \cos \phi_3 \cos \delta, \end{aligned} \quad (6)$$

where  $r_D$  is the ratio of the doubly Cabibbo-suppressed and Cabibbo-allowed  $D^0$  decay ampli-

tudes:

$$r_D = \left| \frac{A(D^0 \rightarrow K^+\pi^-)}{A(D^0 \rightarrow K^-\pi^+)} \right| = 0.060 \pm 0.002, \quad (7)$$

and  $\delta$  is a sum of strong phase differences in  $B$  and  $D$  decays:  $\delta = \delta_B + \delta_D$ .

The update of the ADS analysis using 657M  $B\bar{B}$  pair was recently reported by Belle [8]. The analysis uses  $B^{\pm} \rightarrow DK^{\pm}$  decays with  $D^0$  decaying to  $K^+\pi^-$  and  $K^-\pi^+$  modes (and their charge-conjugated partners). The ratio of the suppressed and allowed modes is

$$\mathcal{R}_{ADS} = (8.0_{-5.7-2.8}^{+6.3+2.0}) \times 10^{-3}. \quad (8)$$

Belle also reports the measurement of the  $CP$  asymmetry, which appears to be consistent with zero:

$$\mathcal{A}_{ADS} = -0.13_{-0.88}^{+0.98} \pm 0.26. \quad (9)$$

The ADS analysis currently does not give a significant constraint on  $\phi_3$ , but it provides an important information on the value of  $r_B$ . Using the conservative assumption  $\cos \phi_3 \cos \delta = -1$  one obtains the upper limit  $r_B < 0.19$  at 90% CL. Somewhat tighter constraint can be obtained by using the  $\phi_3$  and  $\delta_B$  measurements from the Dalitz analyses (see Section 4), and the recent CLEO-c measurement of the strong phase  $\delta_D = (22_{-12-11}^{+11+9})^\circ$  [9].

### 4. Dalitz plot analyses

A Dalitz plot analysis of a three-body final state of the  $D$  meson allows one to obtain all the information required for determination of  $\phi_3$  in a single decay mode. The use of a Dalitz plot analysis for the extraction of  $\phi_3$  was first discussed by D. Atwood, I. Duniety and A. Soni, in the context of the ADS method [7]. This technique uses the interference of Cabibbo-favored  $D^0 \rightarrow K^-\pi^+\pi^0$  and doubly Cabibbo-suppressed  $\bar{D}^0 \rightarrow K^-\pi^+\pi^0$  decays. However, the small rate for the doubly Cabibbo-suppressed decay limits the sensitivity of this technique.

Three body final states such as  $K_S^0\pi^+\pi^-$  [10, 11] have been suggested as promising modes for the extraction of  $\phi_3$ . Like in the GLW or ADS method, the two amplitudes interfere as the  $D^0$  and  $\bar{D}^0$  mesons decay into the same final state  $K_S^0\pi^+\pi^-$ ; we denote the admixed state as  $\bar{D}_+$ . Assuming no  $CP$  asymmetry in neutral  $D$  decays, the amplitude of the  $\bar{D}_+$  decay as a function of Dalitz plot variables  $m_+^2 = m_{K_S^0\pi^+}^2$  and  $m_-^2 = m_{K_S^0\pi^-}^2$  is

$$f_{B^+} = f_D(m_+^2, m_-^2) + r_B e^{i\phi_3 + i\delta_B} f_D(m_-^2, m_+^2), \quad (10)$$

where  $f_D(m_+^2, m_-^2)$  is the amplitude of the  $\bar{D}^0 \rightarrow K_S^0\pi^+\pi^-$  decay.

Similarly, the amplitude of the  $\tilde{D}_-$  decay from  $B^- \rightarrow DK^-$  process is

$$f_{B^-} = f_D(m_-^2, m_+^2) + r_B e^{-i\phi_3 + i\delta_B} f_D(m_+^2, m_-^2). \quad (11)$$

The  $\overline{D}^0 \rightarrow K_S^0 \pi^+ \pi^-$  decay amplitude  $f_D$  can be determined from a large sample of flavor-tagged  $\overline{D}^0 \rightarrow K_S^0 \pi^+ \pi^-$  decays produced in continuum  $e^+e^-$  annihilation. Once  $f_D$  is known, a simultaneous fit of  $B^+$  and  $B^-$  data allows the contributions of  $r_B$ ,  $\phi_3$  and  $\delta_B$  to be separated. The method has only a two-fold ambiguity:  $(\phi_3, \delta_B)$  and  $(\phi_3 + 180^\circ, \delta_B + 180^\circ)$  solutions cannot be distinguished. References [10] and [12] give a more detailed description of the technique.

Both Belle and BaBar collaborations reported recently the updates of the  $\phi_3(\gamma)$  measurements using Dalitz plot analysis. The preliminary result obtained by Belle [13] uses the data sample of 657M  $B\overline{B}$  pairs and two modes,  $B^\pm \rightarrow DK^\pm$  and  $B^\pm \rightarrow D^*K^\pm$  with  $D^* \rightarrow D\pi^0$ . The neutral  $D$  meson is reconstructed in  $K_S^0 \pi^+ \pi^-$  final state in both cases.

To determine the decay amplitude,  $D^{*\pm}$  mesons produced via the  $e^+e^- \rightarrow c\bar{c}$  continuum process are used, which then decay to a neutral  $D$  and a charged pion. The flavor of the neutral  $D$  meson is tagged by the charge of the pion in the decay  $D^{*\pm} \rightarrow \overline{D}^0 \pi^\mp$ .  $B$  factories offer large sets of such charm data:  $290.9 \times 10^3$  events are used in Belle analysis with only 1.0% background.

The description of the  $\overline{D}^0 \rightarrow K_S^0 \pi^+ \pi^-$  decay amplitude is based on the isobar model. The amplitude  $f_D$  is represented by a coherent sum of two-body decay amplitudes and one non-resonant decay amplitude,

$$f_D(m_+^2, m_-^2) = \sum_{j=1}^N a_j e^{i\xi_j} \mathcal{A}_j(m_+^2, m_-^2) + a_{\text{NR}} e^{i\xi_{\text{NR}}}, \quad (12)$$

where  $\mathcal{A}_j(m_+^2, m_-^2)$  is the matrix element,  $a_j$  and  $\xi_j$  are the amplitude and phase of the matrix element, respectively, of the  $j$ -th resonance, and  $a_{\text{NR}}$  and  $\xi_{\text{NR}}$  are the amplitude and phase of the non-resonant component. The model includes a set of 18 two-body amplitudes: five Cabibbo-allowed amplitudes:  $K^*(892)^+ \pi^-$ ,  $K^*(1410)^+ \pi^-$ ,  $K_0^*(1430)^+ \pi^-$ ,  $K_2^*(1430)^+ \pi^-$  and  $K^*(1680)^+ \pi^-$ ; their doubly Cabibbo-suppressed partners; eight amplitudes with  $K_S^0$  and a  $\pi\pi$  resonance:  $K_S^0 \rho$ ,  $K_S^0 \omega$ ,  $K_S^0 f_0(980)$ ,  $K_S^0 f_2(1270)$ ,  $K_S^0 f_0(1370)$ ,  $K_S^0 \rho(1450)$ ,  $K_S^0 \sigma_1$  and  $K_S^0 \sigma_2$ ; and a flat non-resonant term. The free parameters of the fit are the amplitudes  $a_j$  and phases  $\xi_j$  of the resonances, and the amplitude  $a_{\text{NR}}$  and phase  $\xi_{\text{NR}}$  of the non-resonant component. The results of the  $\overline{D}^0 \rightarrow K_S^0 \pi^+ \pi^-$  amplitude fit are shown in Table II.

The selection of  $B^\pm \rightarrow D^{(*)}K^\pm$  decays is based on the CM energy difference  $\Delta E = \sum E_i - E_{\text{beam}}$  and the beam-constrained  $B$  meson mass  $M_{\text{bc}} =$

Table II Fit results for  $\overline{D}^0 \rightarrow K_S^0 \pi^+ \pi^-$  decay. Errors are statistical only.

Intermediate state	Amplitude	Phase ( $^\circ$ )
$K_S \sigma_1$	$1.56 \pm 0.06$	$214 \pm 3$
$K_S \rho^0$	1.0 (fixed)	0 (fixed)
$K_S \omega$	$0.0343 \pm 0.0008$	$112.0 \pm 1.3$
$K_S f_0(980)$	$0.385 \pm 0.006$	$207.3 \pm 2.3$
$K_S \sigma_2$	$0.20 \pm 0.02$	$212 \pm 12$
$K_S f_2(1270)$	$1.44 \pm 0.04$	$342.9 \pm 1.7$
$K_S f_0(1370)$	$1.56 \pm 0.12$	$110 \pm 4$
$K_S \rho^0(1450)$	$0.49 \pm 0.08$	$64 \pm 11$
$K^*(892)^+ \pi^-$	$1.638 \pm 0.010$	$133.2 \pm 0.4$
$K^*(892)^- \pi^+$	$0.149 \pm 0.004$	$325.4 \pm 1.3$
$K^*(1410)^+ \pi^-$	$0.65 \pm 0.05$	$120 \pm 4$
$K^*(1410)^- \pi^+$	$0.42 \pm 0.04$	$253 \pm 5$
$K_0^*(1430)^+ \pi^-$	$2.21 \pm 0.04$	$358.9 \pm 1.1$
$K_0^*(1430)^- \pi^+$	$0.36 \pm 0.03$	$87 \pm 4$
$K_2^*(1430)^+ \pi^-$	$0.89 \pm 0.03$	$314.8 \pm 1.1$
$K_2^*(1430)^- \pi^+$	$0.23 \pm 0.02$	$275 \pm 6$
$K^*(1680)^+ \pi^-$	$0.88 \pm 0.27$	$82 \pm 17$
$K^*(1680)^- \pi^+$	$2.1 \pm 0.2$	$130 \pm 6$
non-resonant	$2.7 \pm 0.3$	$160 \pm 5$

$\sqrt{E_{\text{beam}}^2 - (\sum \vec{p}_i)^2}$ , where  $E_{\text{beam}}$  is the CM beam energy, and  $E_i$  and  $\vec{p}_i$  are the CM energies and momenta of the  $B$  candidate decay products. To suppress background from  $e^+e^- \rightarrow q\bar{q}$  ( $q = u, d, s, c$ ) continuum events, the variables that characterize the event shape are also calculated. At the first stage of the analysis, when the  $(M_{\text{bc}}, \Delta E)$  distribution is fitted in order to obtain the fractions of the background components, the requirement on the event shape is imposed to suppress the continuum events. The number of such ‘‘clean’’ events is 756 for  $B^\pm \rightarrow DK^\pm$  mode with 29% background, and 149 events for  $B^\pm \rightarrow D^*K^\pm$  mode with 20% background. In the Dalitz plot fit, the events are not rejected based on event shape variables, these are used in the likelihood function to better separate signal and background events.

The Dalitz distributions of the  $B^+$  and  $B^-$  samples are fitted separately, using Cartesian parameters  $x_\pm = r_\pm \cos(\pm\phi_3 + \delta_B)$  and  $y_\pm = r_\pm \sin(\pm\phi_3 + \delta_B)$ , where the indices ‘‘+’’ and ‘‘-’’ correspond to  $B^+$  and  $B^-$  decays, respectively. In this approach the amplitude ratios ( $r_+$  and  $r_-$ ) are not constrained to be equal for the  $B^+$  and  $B^-$  samples. Confidence intervals in  $r_B$ ,  $\phi_3$  and  $\delta_B$  are then obtained from the  $(x_\pm, y_\pm)$  using a frequentist technique. The values of the fit parameters  $x_\pm$  and  $y_\pm$  are listed in Table III.

The values of the parameters  $r_B$ ,  $\phi_3$  and  $\delta_B$  obtained from the combination of  $B^\pm \rightarrow DK^\pm$  and  $B^\pm \rightarrow D^*K^\pm$  modes are presented in Table IV. Note that in addition to the detector-related systematic error which is caused by the uncertainties of the back-

Table III Results of the signal fits in parameters  $(x, y)$ . The first error is statistical, the second is experimental systematic error. Model uncertainty is not included.

Parameter	$B^+ \rightarrow DK^+$	$B^+ \rightarrow D^*K^+$
$x_-$	$+0.105 \pm 0.047 \pm 0.011$	$+0.024 \pm 0.140 \pm 0.018$
$y_-$	$+0.177 \pm 0.060 \pm 0.018$	$-0.243 \pm 0.137 \pm 0.022$
$x_+$	$-0.107 \pm 0.043 \pm 0.011$	$+0.133 \pm 0.083 \pm 0.018$
$y_+$	$-0.067 \pm 0.059 \pm 0.018$	$+0.130 \pm 0.120 \pm 0.022$

ground description, imperfect simulation etc., the result suffers from the uncertainty of the  $D$  decay amplitude description. The statistical confidence level of  $CP$  violation for the combined result is  $(1-5.5 \times 10^{-4})$ , or 3.5 standard deviations.

In contrast to Belle analysis, BaBar [14] uses a smaller data sample of 383M  $B\bar{B}$  pairs, but analyses seven different decay modes:  $B^\pm \rightarrow DK^\pm$ ,  $B^\pm \rightarrow D^*K^\pm$  with  $D^0 \rightarrow D\pi^0$  and  $D\gamma$ , and  $B^\pm \rightarrow DK^{*\pm}$ , where the neutral  $D$  meson is reconstructed in  $K_S^0\pi^+\pi^-$  and  $K_S^0K^+K^-$  (except for  $B^\pm \rightarrow DK^{*\pm}$  mode) final states. The signal yields for these modes are shown in Table V.

The differences from the Belle model of  $\bar{D}^0 \rightarrow K_S^0\pi^+\pi^-$  decay are as follows: the K-matrix formalism is used by default to describe the  $\pi\pi$   $S$ -wave, while the  $K\pi$   $S$ -wave is parametrized using  $K_0^*(1430)$  resonances and an effective range non-resonant component with a phase shift.

The description of  $\bar{D}^0 \rightarrow K_S^0K^+K^-$  decay amplitude uses an isobar model with eight two-body decays:  $K_S^0a_0(980)^0$ ,  $K_S^0\phi(1020)$ ,  $K_S^0f_0(1370)$ ,  $K_S^0f_2(1270)^0$ ,  $K_S^0a_0(1450)^0$ ,  $K^-a_0(980)^+$ ,  $K^+a_0(980)^-$ , and  $K^-a_0(1450)^+$ . The results of the  $\bar{D}^0 \rightarrow K_S^0K^+K^-$  amplitude fit are shown in Table VI.

The fit to signal samples is performed in a similar way as in Belle analysis, using the unbinned likelihood function that includes Dalitz plot variables,  $B$  meson selection variables, and event shape parameters. The results of the fit in Cartesian parameters are shown in Table VII. In the combination of all modes, BaBar obtains  $\gamma = (76_{-24}^{+23} \pm 5 \pm 5)^\circ$  (mod  $180^\circ$ ). The values of the amplitude ratios are  $r_B = 0.086 \pm 0.035 \pm 0.010 \pm 0.011$  for  $B^\pm \rightarrow DK^\pm$ ,  $r_B^* = 0.135 \pm 0.051 \pm 0.011 \pm 0.005$  for  $B^\pm \rightarrow D^*K^\pm$ , and  $\kappa r_s = 0.163_{-0.105}^{+0.088} \pm 0.037 \pm 0.021$  for  $B^\pm \rightarrow DK^{*\pm}$  (here  $\kappa$  accounts for possible nonresonant  $B^\pm \rightarrow DK_S^0\pi^\pm$  contribution). The significance of the direct  $CP$  violation is 99.7%, or 3.0 standard deviations.

## 5. Other techniques

Several other decays involving neutral  $B$  mesons have been tried by BaBar collaboration for  $\gamma$  measurement. One of them is the decay  $B^0 \rightarrow DK^*(892)^0$ ,

where the similar Dalitz analysis of the three-body decay  $\bar{D}^0 \rightarrow K_S^0\pi^+\pi^-$  is performed. Similarly to  $B^\pm \rightarrow DK^\pm$  decays, this mode allows for direct measurement of the angle  $\gamma$ , but since both amplitudes involving  $D^0$  and  $\bar{D}^0$  are color-suppressed, the value of  $r_B$  is larger  $r_B \sim 0.4$ . The flavor of the  $B$  meson is tagged by the charges of the  $K^*(892)^0$  decay products ( $K^+\pi^-$  or  $K^-\pi^+$ ).

The analysis based on 371M  $B\bar{B}$  pairs was performed [15]. The analysis procedure is similar to that with charged  $B$  mesons. The fit yields the following constraints on  $\gamma$  and amplitude ratio  $r_B$ :  $\gamma = (162 \pm 56)^\circ$ ,  $r_B < 0.55$  with 90% CL.

Another neutral  $B$  decay mode investigated by BaBar is  $B^0 \rightarrow D^\mp K^0\pi^\pm$ . Similarly to measurements based on  $B^0 \rightarrow D^{(*)}\pi$  decays [16, 17], the interference between the  $b \rightarrow u$  and  $b \rightarrow c$  diagrams is achieved due to the mixing of neutral  $B$  mesons. Therefore, this method requires to tag the flavor of the other  $B$  meson and to perform a time-dependent analysis. As a result, this method is sensitive to the combination  $2\beta + \gamma$  of the CKM angles [18, 19].

First advantage of this technique compared to the methods based on  $B^0 \rightarrow D^{(*)}\pi$  decays is that, since both  $b \rightarrow c$  and  $b \rightarrow u$  diagrams involved in this decay are color-suppressed, the expected value of the ratio  $r$  is of the order 0.3. Secondly,  $2\beta + \gamma$  is measured with only a two-fold ambiguity (compared to four-fold in  $B^0 \rightarrow D^{(*)}\pi$  decays). In addition, all strong amplitudes and phases can be, in principle, measured in the same data sample.

The BaBar collaboration has performed the analysis based on 347M  $B\bar{B}$  pairs data sample [20]. Time-dependent Dalitz plot analysis of the decay  $B^0 \rightarrow D^\mp K^0\pi^\pm$  is performed. This decay is found to be dominated by  $B^0 \rightarrow D^{*0}K_S^0$  (both  $b \rightarrow u$  and  $b \rightarrow c$  transitions) and  $B^0 \rightarrow D^-K^{*+}$  ( $b \rightarrow c$ ) states. The analysis finds  $558 \pm 34$  flavor-tagged signal events, from the unbinned maximum likelihood fit to the time-dependent Dalitz distribution, the central value of the  $2\beta + \gamma$  as a function of  $r$  is obtained. The value of  $r$  cannot be fixed with the current data sample, therefore, the value  $r = 0.3$  is used, and its error is taken into account in the systematic error. This results in the value  $2\beta + \gamma = (83 \pm 53 \pm 20)^\circ$  or  $(263 \pm 53 \pm 20)^\circ$ .

## 6. World average results

The world average  $\phi_3$  results that include the latest measurements presented in 2008, are available from UTfit group [21]. The probability density functions for  $\gamma$  and amplitude ratios  $r_B$  are shown in Fig. 2. The world average values for these parameters are  $\phi_3/\gamma = (81 \pm 13)^\circ$ ,  $r_B(DK) = 0.098 \pm 0.017$ ,  $r_B(D^*K) = 0.092 \pm 0.038$ ,  $r_B(DK^*) = 0.13 \pm 0.09$ .

Essential is the fact that for the first time the value of  $r_B$  is shown to be significantly non-zero. In previous

Table IV Results of the combination of  $B^+ \rightarrow DK^+$  and  $B^+ \rightarrow D^*K^+$  modes.

Parameter	$1\sigma$ interval	$2\sigma$ interval	Systematic error	Model uncertainty
$\phi_3$	$76^\circ \begin{smallmatrix} +12^\circ \\ -13^\circ \end{smallmatrix}$	$49^\circ < \phi_3 < 99^\circ$	$4^\circ$	$9^\circ$
$r_{DK}$	$0.16 \pm 0.04$	$0.08 < r_{DK} < 0.24$	0.01	0.05
$r_{D^*K}$	$0.21 \pm 0.08$	$0.05 < r_{D^*K} < 0.39$	0.02	0.05
$\delta_{DK}$	$136^\circ \begin{smallmatrix} +14^\circ \\ -16^\circ \end{smallmatrix}$	$100^\circ < \delta_{DK} < 163^\circ$	$4^\circ$	$23^\circ$
$\delta_{D^*K}$	$343^\circ \begin{smallmatrix} +20^\circ \\ -22^\circ \end{smallmatrix}$	$293^\circ < \delta_{D^*K} < 389^\circ$	$4^\circ$	$23^\circ$

Table V Signal yields of different modes used for Dalitz analysis by BaBar collaboration [14].

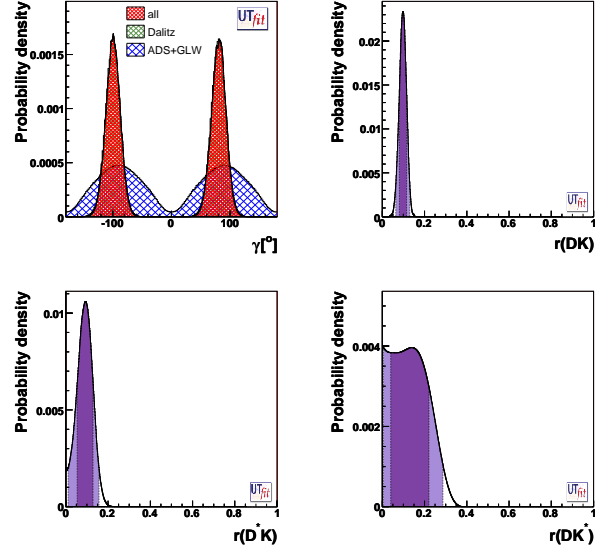
$B$ decay	$D$ decay	Yield
$B^\pm \rightarrow DK^\pm$	$\overline{D}^0 \rightarrow K_S^0 \pi^+ \pi^-$	$600 \pm 31$
	$\overline{D}^0 \rightarrow K_S^0 K^+ K^-$	$112 \pm 13$
$B^\pm \rightarrow [D\pi^0]_{D^*} K^\pm$	$\overline{D}^0 \rightarrow K_S^0 \pi^+ \pi^-$	$133 \pm 15$
	$\overline{D}^0 \rightarrow K_S^0 K^+ K^-$	$32 \pm 7$
$B^\pm \rightarrow [D\gamma]_{D^*} K^\pm$	$\overline{D}^0 \rightarrow K_S^0 \pi^+ \pi^-$	$129 \pm 16$
	$\overline{D}^0 \rightarrow K_S^0 K^+ K^-$	$21 \pm 7$
$B^\pm \rightarrow DK^{*\pm}$	$\overline{D}^0 \rightarrow K_S^0 \pi^+ \pi^-$	$118 \pm 18$

 Table VI  $CP$  eigenstates, CA, and DCS complex amplitudes  $a_r e^{i\phi_r}$  and fit fractions, obtained from the fit of the  $D^0 \rightarrow K_S^0 K^+ K^-$  Dalitz plot distribution from  $D^{*+} \rightarrow D^0 \pi^+$ . Errors are statistical only.

Component	$\Re\{a_r e^{i\phi_r}\}$	$\Im\{a_r e^{i\phi_r}\}$	Frac. (%)
$K_S^0 a_0(980)^0$	1	0	55.8
$K_S^0 \phi(1020)$	$-0.126 \pm 0.003$	$0.189 \pm 0.005$	44.9
$K_S^0 f_0(1370)$	$-0.04 \pm 0.06$	$-0.00 \pm 0.05$	0.1
$K_S^0 f_2(1270)$	$0.257 \pm 0.019$	$-0.041 \pm 0.026$	0.3
$K_S^0 a_0(1450)^0$	$0.06 \pm 0.12$	$-0.65 \pm 0.09$	12.6
$K^- a_0(980)^+$	$-0.561 \pm 0.015$	$0.01 \pm 0.03$	16.0
$K^- a_0(1450)^+$	$-0.11 \pm 0.06$	$0.81 \pm 0.03$	21.8
$K^+ a_0(980)^-$	$-0.087 \pm 0.016$	$0.079 \pm 0.014$	0.7

measurements, poor  $r_B$  constraint caused sufficiently non-gaussian errors for  $\phi_3$ , and made it difficult to predict the future sensitivity of this parameter. Now that  $r_B$  is constrained to be of the order 0.1, one can confidently extrapolate the current precision to future measurements at LHCb and Super-B facilities.

As it can be seen from Fig. 2 (top left), the  $\phi_3/\gamma$  precision is mainly dominated by Dalitz analyses. These analyses have currently a hard-to-control uncertainty due to  $D^0$  decay amplitude description, which is estimated to be 5–10°. At the current level of statistical precision this error starts to influence the total  $\phi_3/\gamma$  uncertainty. A solution to this problem can be the use of quantum-correlated  $D\overline{D}$  decays at  $\psi(3770)$  resonance available currently at CLEO-c experiment, where the missing information about the strong phase in  $D^0$  decay can be obtained experimentally [22, 23]. With CLEO-c data sample, the  $\gamma$  uncertainty due to


 Figure 2: Probability density functions for  $\phi_3/\gamma$  (top left), and  $r_B$  in  $B^\pm \rightarrow DK^\pm$  (top right),  $B^\pm \rightarrow D^*K^\pm$  (bottom left), and  $B^\pm \rightarrow DK^{*\pm}$  (bottom right) based on all available  $\phi_3/\gamma$  measurements.

$D$  decay amplitude can be as low as 5° (and, since it becomes a statistical uncertainty, it is more reliable than the current estimation based on the arbitrary variations of the model), while with the future BES-III sample it can be lowered to a degree level.

UTfit constraints on the Unitarity Triangle vertex are shown in Fig. 3. The plot shows a good agreement between the different measurements, and  $\phi_3/\gamma$  results, although still have poorer sensitivity compared to other angles measurements, fit well into the whole picture.

## 7. Conclusion

In the past year, many new measurements related to determination of  $\phi_3/\gamma$  have appeared. As a result, strong evidence of a direct  $CP$  violation in  $B^\pm \rightarrow DK^\pm$  decays is obtained for the first time in a combination of B-factories results. Essential is that the amplitude ratio  $r_B$ , which determines the magnitude of the  $CP$  violation and the precision of the

Table VII  $CP$ -violating parameters  $x_{\mp}^{(*)}$ ,  $y_{\mp}^{(*)}$ ,  $x_{s\mp}$ , and  $y_{s\mp}$ , as obtained from the  $CP$  fit. The first error is statistical, the second is experimental systematic uncertainty and the third is the systematic uncertainty associated with the Dalitz models.

Parameters	$B^- \rightarrow \tilde{D}^0 K^-$	$B^- \rightarrow \tilde{D}^{*0} K^-$	$B^- \rightarrow \tilde{D}^0 K^{*-}$
$x_- , x_-^* , x_{s-}$	$0.090 \pm 0.043 \pm 0.015 \pm 0.011$	$-0.111 \pm 0.069 \pm 0.014 \pm 0.004$	$0.115 \pm 0.138 \pm 0.039 \pm 0.014$
$y_- , y_-^* , y_{s-}$	$0.053 \pm 0.056 \pm 0.007 \pm 0.015$	$-0.051 \pm 0.080 \pm 0.009 \pm 0.010$	$0.226 \pm 0.142 \pm 0.058 \pm 0.011$
$x_+ , x_+^* , x_{s+}$	$-0.067 \pm 0.043 \pm 0.014 \pm 0.011$	$0.137 \pm 0.068 \pm 0.014 \pm 0.005$	$-0.113 \pm 0.107 \pm 0.028 \pm 0.018$
$y_+ , y_+^* , y_{s+}$	$-0.015 \pm 0.055 \pm 0.006 \pm 0.008$	$0.080 \pm 0.102 \pm 0.010 \pm 0.012$	$0.125 \pm 0.139 \pm 0.051 \pm 0.010$

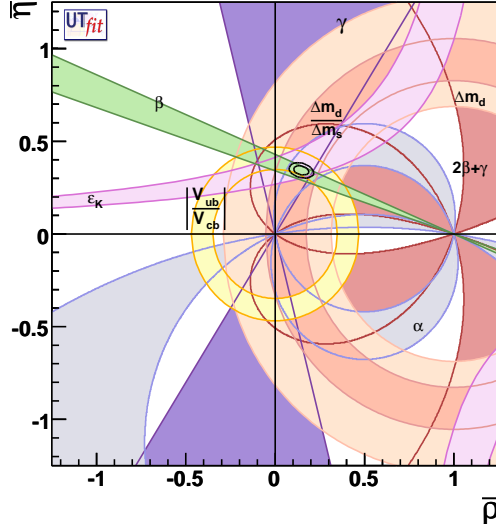


Figure 3: UTfit constraints on the Unitarity Triangle vertex including the latest  $\phi_3/\gamma$  measurements.

$\phi_3/\gamma$  measurement, is finally constrained to be non-zero ( $r_B = 0.10 \pm 0.02$  in the UTfit world average). This allows to confidently extrapolate the sensitivity of  $\phi_3/\gamma$  measurements to future experiments. Current world average is  $\phi_3/\gamma = (81 \pm 13)^\circ$ ; this value is dominated by the measurements based on Dalitz plot analyses of  $D$  decay from  $B^\pm \rightarrow D^{(*)}K^{(*)\pm}$  precesses. Although these analyses currently include a hard-to-control uncertainty due to the  $D$  decay model, there are ways of dealing with this problem using charm data samples from CLEO-c and BES-III facilities, that should allow for a degree-level precision of  $\phi_3/\gamma$  to be reached at the next generation  $B$  factories.

## References

- [1] BaBar Collaboration, B. Aubert *et al.*, Phys. Rev. D **71**, 032005 (2005).
- [2] Belle Collaboration, R. Itoh, Y. Onuki *et al.*, Phys. Rev. Lett. **95** 091601 (2005).
- [3] M. Gronau, D. London, D. Wyler, Phys. Lett. B **253**, 483 (1991); M. Gronau, D. London, D. Wyler, Phys. Lett. B **265**, 172 (1991)
- [4] BaBar collaboration, B. Aubert *et al.*, Nucl. Instrum. Meth. A **479**, 1 (2002).
- [5] Belle collaboration, A. Abashian *et al.*, Nucl. Instrum. Meth. A **479**, 117 (2002).
- [6] BaBar collaboration, B. Aubert *et al.*, arXiv:0802.4052
- [7] D. Atwood, I. Dunietz, A. Soni, Phys. Rev. Lett. **78**, 3357 (1997)
- [8] Belle collaboration, Y. Horii *et al.*, arXiv:0804.2063
- [9] CLEO collaboration, D. M. Asner *et al.*, arXiv:0802.2268
- [10] A. Giri, Yu. Grossman, A. Soffer, J. Zupan, Phys. Rev. D **68**, 054018 (2003).
- [11] A. Bondar. Proceedings of BINP Special Analysis Meeting on Dalitz Analysis, 24-26 Sep. 2002, unpublished.
- [12] Belle Collaboration, A. Poluektov *et al.*, Phys. Rev. D **73**, 112009 (2006).
- [13] Belle collaboration, K. Abe *et al.*, arXiv:0803.3375
- [14] BaBar collaboration, B. Aubert *et al.*, arXiv:0804.2089
- [15] V. Sordini, talk at Rencontres de Moriond 2008, Electroweak session.
- [16] BaBar collaboration, B. Aubert *et al.*, Phys. Rev. D **71**, 112003 (2005)
- [17] Belle collaboration, T. Gershon *et al.*, Phys. Lett. B **624**, 11 (2005).
- [18] R. Aleksan, T.C. Petersen, A. Soffer, Phys. Rev. D **67** (2003) 096002
- [19] F. Polci, M.-H. Schune, A. Stocchi, arXiv:hep-ph/0605129
- [20] BaBar collaboration, B. Aubert *et al.*, arXiv:0712.3469
- [21] <http://www.utfit.org>
- [22] A. Bondar and A. Poluektov, Eur. Phys. J. C **47**, 347 (2006).
- [23] A. Bondar and A. Poluektov, Eur. Phys. J. C **55**, 51 (2008).